

# Intelligent Chest X-ray Worklist Prioritization by CNNs: A Clinical Workflow Simulation

**Ivo M. Baltruschat**<sup>1,2,3,4</sup>

I.BALTRUSCHAT@UKE.DE

<sup>1</sup> *Department for Diagnostic and Interventional Radiology and Nuclear Medicine, University Medical Center Hamburg-Eppendorf, Hamburg, Germany*

<sup>2</sup> *Institute for Biomedical Imaging, Hamburg University of Technology, Hamburg, Germany*

<sup>3</sup> *Philips Research, Hamburg, Germany*

<sup>4</sup> *DAISYLab, Forschungszentrum Medizintechnik Hamburg, Hamburg, Germany*

**Leonhard Steinmeister**<sup>1,4</sup>

**Hannes Nickisch**<sup>3</sup>

**Axel Saalbach**<sup>3</sup>

**Michael Grass**<sup>3</sup>

**Gerhard Adam**<sup>1</sup>

**Harald Ittrich**<sup>1</sup>

**Tobias Knopp**<sup>1,2</sup>

## Abstract

Growing radiologic workload and shortage of medical experts worldwide often lead to delayed or even unreported examinations, which poses a risk for patients safety in case of unrecognized findings in chest radiographs (CXR). The aim was to evaluate, whether deep learning algorithms for an intelligent worklist prioritization might optimize the radiology workflow and can reduce report turnaround times (RTAT) for critical findings, instead of reporting according to the First-In-First-Out-Principle (FIFO). Furthermore, we investigated the problem of false negative prediction in the context of worklist prioritization.

To assess the potential benefit of an intelligent worklist prioritization, three different workflow simulations based on our analysis were run and RTAT were compared: FIFO (non-prioritized), Prio1 (prioritized) and Prio2 (prioritized, with RTATmax.). Examination triage was performed by “ChestXCheck”, a convolutional neural network, classifying eight different pathological findings ranked in descending order of urgency: pneumothorax, pleural effusion, infiltrate, congestion, atelectasis, cardiomegaly, mass and foreign object.

The average RTAT for all critical findings was significantly reduced by both Prio simulations compared to the FIFO simulation (e.g. pneumothorax: 32.1 min vs. 69.7 min;  $p < 0.0001$ ), while the average RTAT for normal examinations increased at the same time (69.5 min vs. 90.0 min;  $p < 0.0001$ ). Both effects were slightly lower at Prio2 than at Prio1, whereas the maximum RTAT at Prio1 was substantially higher for all classes, due to individual examinations rated false negative.

Our Prio2 simulation demonstrated that intelligent worklist prioritization by deep learning algorithms reduces average RTAT for critical findings in chest X-ray while maintaining a similar maximum RTAT as FIFO.

## 1. Introduction

Growing radiologic workload, shortage of medical experts and declining revenues often lead to potentially dangerous backlogs of unreported examinations, especially in publicly funded health care systems. With the increasing demand for radiological imaging, the continuous acceleration of image acquisition and the expansion of teleradiological care, radiologists are nowadays working under increasing pressure of time, which cannot be compensated by improving RIS-PACS integration or use of speech recognition software [1].

However, late communication of critical findings to the referring physician bears the risk of delayed clinical intervention and impairs the outcome of medical treatment [2-4], especially in cases that require immediate action, e.g. tension pneumothorax or misplaced catheters. Therefore, the Joint Commission defined timely reporting of critical diagnostic results as one important goal for patient's safety [5].

Many institutions process their examination worklists still following the First-In-First-Out (FIFO) principle. The urgency information provided by the ordering physician is often incomplete or presented as ambiguous and ill-defined priority level, such as "critical", "ASAP" or "STAT" [6]. A recent study related to portable chest radiographs, reported that 38% of all STAT exams were not clinically urged [7].

While rule-based approaches, that assign cases to specific worklists (e.g. ED or sub-specialty), can help to optimize the overall workflow, they can't take imaging findings into account. The prioritization by the radiographers after the acquisition has not found any application in the clinical routine.

Deep Learning techniques such as Convolutional Neural Networks (CNN) offer promising options to facilitate the clinical workflow. Automated disease classification systems based on CNNs can enable a real-time prioritization of worklists and reduce the report turnaround time (RTAT) for critical findings by up to 60% demonstrated for head and neck CTs [8]. For most common conventional chest X-ray examinations (CXR) a potential benefit of real-time triaging by CNNs has been reported by Annarumma et al [9], but this study focused mostly on the development of an AI system without a real clinical simulation and does not present maximum RTAT for critical findings.

In this work, we simulate multiple intelligent CXR worklist prioritization methods in a realistic clinical setting, using empirical data from the University Medical Center Hamburg-Eppendorf (UKE). The aim was to evaluate, whether deep learning algorithms for an intelligent worklist prioritization might optimize the radiology workflow by reducing RTAT for critical findings, instead of FIFO reporting. Furthermore, we investigated the problem of false negative prediction in the context of worklist prioritization.

## 2. Material & Methods

### 2.1. Convolutional Neural Network Architecture

Based on previous work [10,11] we employ a tailored ResNet-50 architecture with a larger input size of 448 x 448, trained on the publicly available ChestX-ray14 dataset [12]. After replacing the last dense layer of the converged model, the network was fine-tuned on the publicly available Indiana dataset [13], containing 3996 CXRs. All examinations were annotated by two expert radiologists from our department regarding eight different classes:

pneumothorax, congestion, pleural effusion, infiltrate, atelectasis, cardiomegaly, mass, foreign object and “no pathological finding”. For the annotation process, both, frontal and lateral views were employed, while only the frontal views were subject to the CNN-based classification.

Furthermore, the CXRs were preprocessed by two different methods before training (i.e. lung field segmentation and bone suppression), as shown in earlier experiments the highest average AUC value was achieved by combining both methods by ensembling [11]. Due to the importance of pneumothorax detection and the low number of cases with “pneumothorax” in our training dataset ( $n=11$ ) a version of ResNet-50, trained specifically for the detection of pneumothorax, was employed in the following [14]. The final model “ChestXCheck” obtained the highest average AUC value (Figure 1) in previous experiments compared to different network architectures.

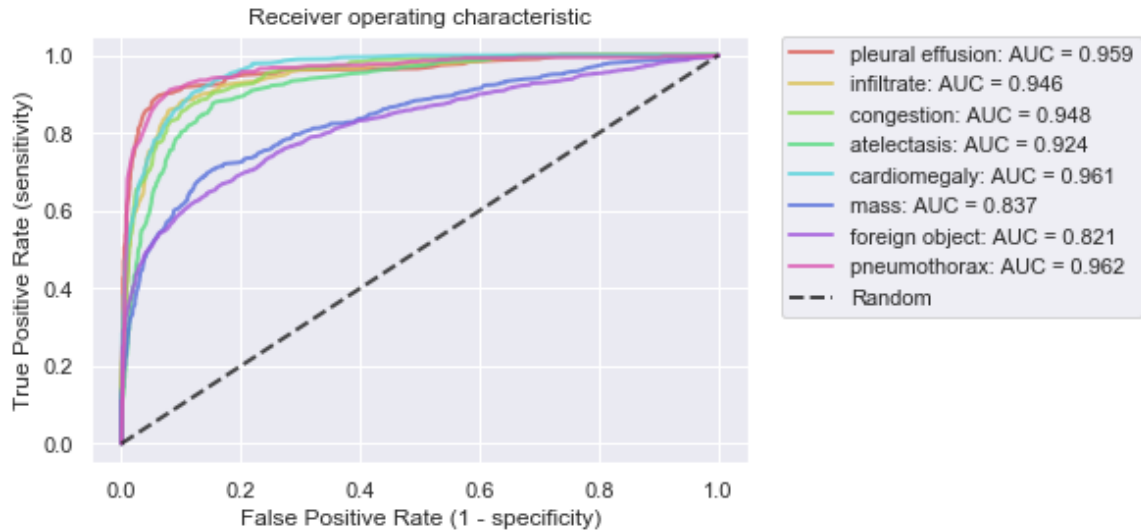


Figure 1: Receiver operating characteristics of the “ChestXCheck” AI algorithm for all eight different classes.

## 2.2. Pathology Triage

For triage, a ranking of the pathologies was defined by two experienced radiologists, reflecting the urgency for clinical action. As our annotations did not include different degrees of pathology manifestation, only the presence of a pathology was considered for the prioritization. Furthermore, the impact of different pathology combinations was not considered. The following eight different pathological findings are ranked in descending order of urgency: pneumothorax, pleural effusion, infiltrate, congestion, atelectasis, cardiomegaly, mass and foreign object.

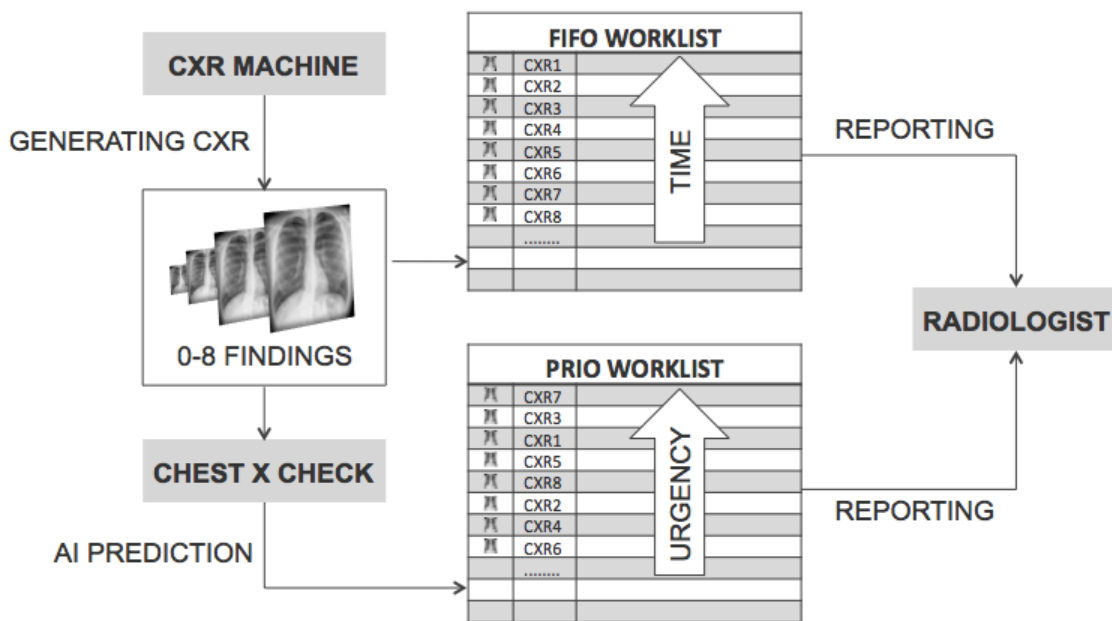


Figure 2: Workflow Simulation. A CXR machine is constantly generating CXRs. To each CXR, zero or up to eight findings are assigned. CXRs are either sorted into the worklist chronologically (FIFO) or according to the urgency based on the prediction by the “ChestXCheck” algorithm (PRIO). Finally, worklists are processed by a virtual radiologist.

### 2.3. Workflow Simulation

To evaluate the clinical effect of a CXR worklist rearrangement by CNNs under realistic conditions, we analyzed the current workflow in the radiology department of the UKF and transferred this data into a computer simulation (Figure 2). We designed a model consisting of four main parts. First, a discrete distribution of how often CXRs are generated. Secondly, the department specific disease prevalence for our eight findings to assign labels to the CXRs. Thirdly, the performance for all eight findings of a state-of-the-art CNN to classify each CXR. Fourthly, a second discrete distribution of how fast a radiologist finalizes a report for a CXR.

By monitoring the CXR acquisition and reporting process during one week from Monday 00:00 AM until Sunday 00:00 PM (760 examinations in total), we were able to extract a discrete distribution of the acquisition and reporting times of subsequent CXRs to calculate the RTAT [15]. The department specific distribution of pathologies was analyzed by manually annotating all eight findings in 300 CXRs.

To simulate the clinical workload throughout the day, a model of a CXR machine was developed, constantly generating new examinations filling up a worklist. Generation time was sampled from the discrete distribution of our acquisition time analysis (Figure 3), including all effects such as different patient frequency during day and night.

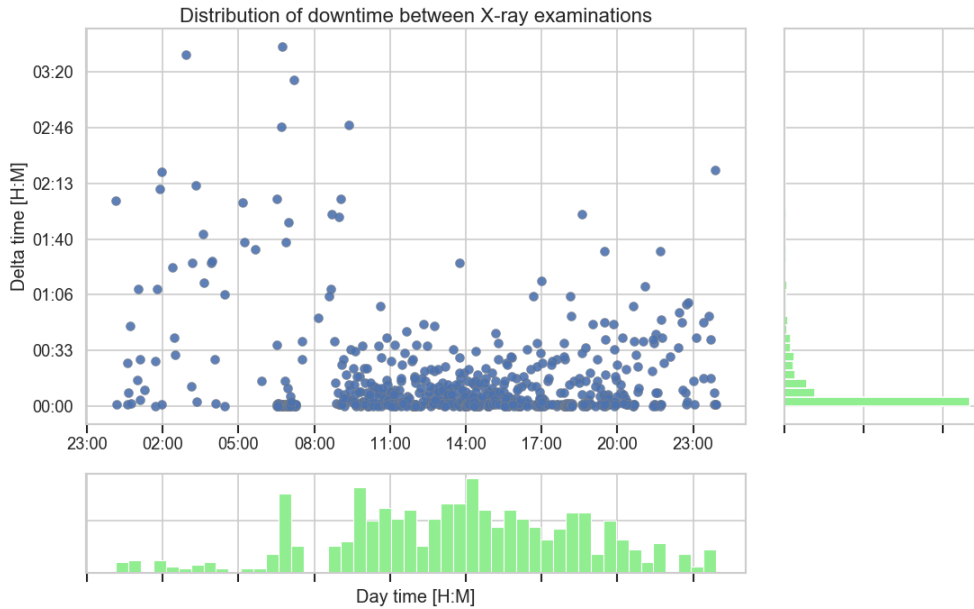


Figure 3: Discrete distribution of CXR generation speed. The X-axis shows the day time in 24-hour format and the Y-axis shows the calculated time deltas. In green, we show the histogram in X- and Y-direction.

Afterwards, pathologies were randomly assigned to the generated images, based on the a-priority probabilities derived from the disease prevalence at the UKE.

Finally, a model of a radiologist was set up, simultaneously working through the worklist by reporting CXRs on the basis of the FIFO principle and with a speed matching our CXR reporting time analysis. We sampled the reporting speed from our discrete distribution (Figure 4), that included not only the raw reporting speed for a CXR but also other factors including pauses or interruptions due to phone calls. This simulation model (FIFO), resembling the current clinical workflow, was compared to the prioritization model (Prio1), applying "ChestXCheck" to all CXRs before sorting the examinations into the worklist.

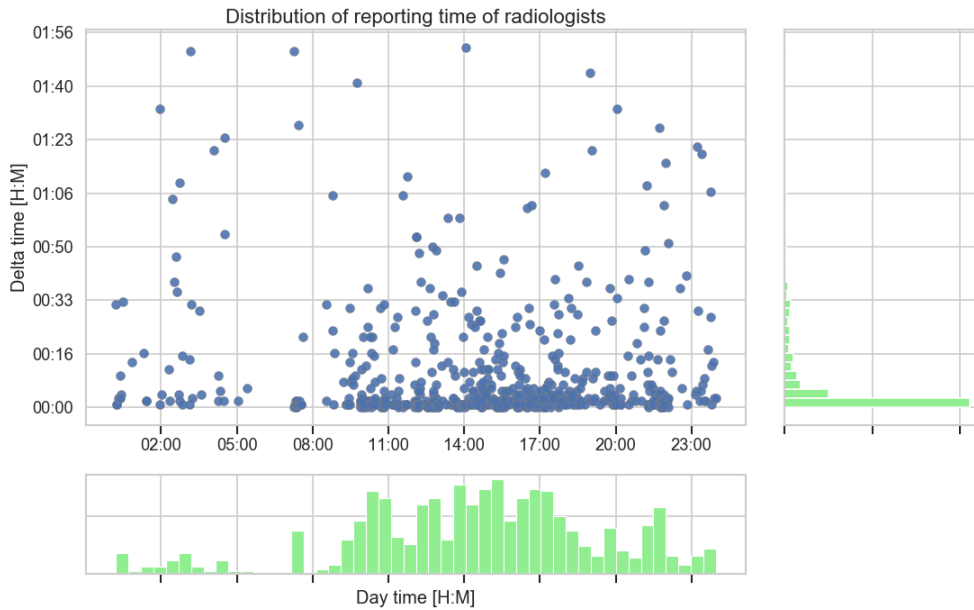


Figure 4: Discrete distribution of CXR reporting times by radiologists. The X-axis shows the day time in 24-hour format and the Y-axis shows the calculated time deltas between two CXR reports. In green, we show the histogram in X- and Y-direction.

By automatically predicting the presence of all eight pathological findings an urgency level could be assigned. Depending on the estimated level, the image was inserted into the existing worklist, taking prior images with a similar or higher level into account. The rearranged worklist was processed by the same radiologist model as in the FIFO simulation. In our evaluation, we compared the average and the maximum RTAT of both simulations.

Finally, we also employed a third scheduling model (Prio2) with a threshold for the maximum waiting time. While the previous strategy favors cases based on the CNN prediction, in rare situations, erroneous result could result in a significantly increased RTAT for studies with an undetected critical finding. Therefore, we developed an alternative method

with a maximum wait time for each examination. After a maximum waiting time of 600 min based on the maximum at the FIFO simulation, the examination was assigned with the highest priority to reduce the problem caused by false negative predictions.

All methods were tested using a Monte-Carlo simulation over 10.000 days with 24 hours of clinical routine, covering the generation of about 1.000.000 CXRs. Furthermore, the worklist was completed at the end of the day in all simulation.

### 3. Results

#### 3.1. Optimal operation point on the ROC-Curve

When employing AI multi-label classification, a threshold for every pathology must be defined in order to derive a binary classification from the continuous response of the system. This corresponds to the selection of an operation point on the ROC curve taking into account two factors. First, what is the best tradeoff between the true positive and false positive rate with respect to the RTAT. While an exhaustive valuation of different thresholds for all pathologies is computationally prohibitive, we focused on pneumothorax only (the most critical finding in our setting). Here, we estimated the RTAT for different operating points by sampling the ROC curve at different false positive rates. As shown in Figure 5, higher false positive rated reduces the effect of intelligent worklist prioritization to almost zero i.e. almost all examinations are rate urged. While the other extreme (i.e. low false positive rate with low true positive), can have no effect either, if almost all image are rated non-urged. Secondly, the false negative rate, since sorting individual examinations with critical findings to the end of the worklist bears severe risks of delayed treatment.

We chose the optimal operation point on the AUC curve for all pathologies based on our results in Figure 5. Hence, we set the false positive rate to 0.05 for all findings without a relevant increase in the average RTAT.

#### 3.2. Pathology Distribution

The analysis of pathology distribution at the UKE was extracted by manually annotating 300 CXR reports from February 2019 by an expert radiologist. Due to a mainly stationary patient collective from a hospital of maximum care the portion of CXR without pathological findings was only 33%. The prevalence of the most critical finding "pneumothorax" was around 5%. Results are demonstrated in Table 1.

#### 3.3. CXR Generation and Reporting Time Analysis

We used a total of 760 examinations to determine a discrete distribution of CXR generation and radiologists reporting speed. For CXR generation speed, we used the creation timestamp of two consecutive CXRs to calculate the delta between their creation. The delta represents the acquisition rate of CXRs at the institution. We employed the same method for the reporting speed. Here we used the report finalization timestamp to determine the delta between two CXRs. Afterwards, we removed all deltas greater than 1h 30min, because we only want outliers in one of the two distributions.

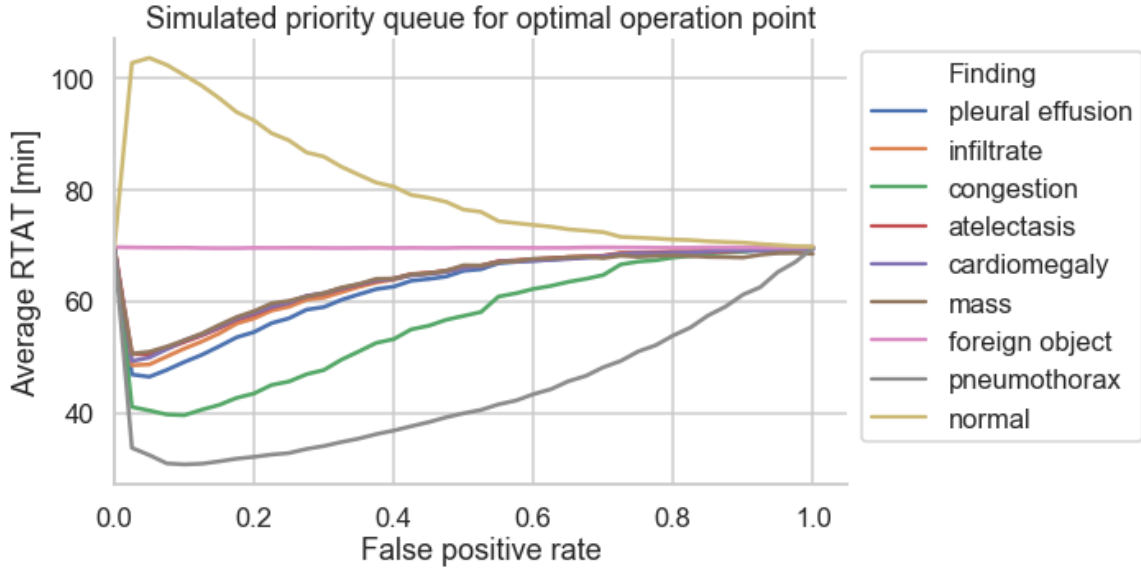


Figure 5: Optimal operation point simulation for the “ChestXCheck” AI algorithm. To find the optimal operation point for reducing the average report turnaround times (RTAT) for critical findings, we run multiple simulation with different the false positive rates between zero and one.

Table 1: Finding prevalence in CXRs at the UKE (approximation by 300 samples from February 2019). The table is ordered by finding urgency.

Finding	Total count	Prevalence [%]
Pneumothorax	14	4.7
Congestion	68	22.7
Pleural effusion	147	49.0
Infiltrate	53	17.7
Atelectasis	77	25.7
Cardiomegaly	42	14.0
Mass	10	3.3
Foreign Object	181	60.3
Normal	98	32.7

### 3.4. Report Turnaround Time Analysis

The average RTAT for a CXR, measured over one week (760 examinations), was 71 min with a range between 1 min and 316 min. Assuming that a CXR report by an experienced radiologist will only take several minutes, this range in reporting time can be explained by different external influences, such as night shifts, change of shifts, working breaks or backlogs.

### 3.5. Workflow Simulations

Figure 6 summarizes the effect of all three simulations (i.e. FIFO, Prio1, Prio2) on the RTAT. The average RTAT for critical findings was significantly reduced in the Prio1 simulation compared to the FIFO simulation e.g. pneumothorax: 32.1 min vs. 69.7 min, congestion: 44.2 min vs. 69.7 min, pleural effusion: 56.0 min vs. 69.7 min. As expected, an increase of average RTAT was only reported for normal examinations with a significant increase of the average RTAT from 69.5 min to 90.0 min. At the same time, however, the maximum RTAT in the Prio1 simulation increased compared to the FIFO simulation for all eight findings (e.g. pneumothorax: 11h 37 min vs. 14 h 55 min), as some examinations were predicted as false negative and sorted to the end of the worklist. In the Prio2 simulation, we countered this problem by a maximum waiting time and reduced the maximum RTAT for most findings (e.g. for pneumothorax from 14 h 55 min to 11h 34 min). While, the average RTAT was only slightly higher than the Prio1 simulation (e.g. pneumothorax: 32.7 min vs. 32.1 min). Finally, we also simulated the upper limit for an intelligent worklist prioritization by virtually employing a perfect classification algorithm (Perfect) with a sensitivity and specificity of one. Table 2 shows the comparison to the other three simulations. For pneumothorax, the Prio2 average RTAT is only 5.9 min slower compared to the Perfect-simulation while FIFO is 42.9 min slower.

### 3.6. Statistical Analysis

The predictive performance of the CNN was assessed by using the area under the receiver operating characteristic curve (AUC). The shown AUC results are averaged over a ten times re-sampling and presented with standard deviation (SD).

We used the Welch's t-test for the significant assessment of our intelligent worklist prioritization. First, we simulated a null distribution for the RTAT where examinations are sorted by the FIFO principle (i.e. random order). Secondly, we also simulated an alternative distribution with worklist prioritization. Both distributions are then used to determine whether the average RTAT for each finding has changed significantly by calculating the p-value with the Welch t-test. Each distribution is simulated with a sample size of 1.000.000 examinations and the significant level is set to 0.05. For all findings except "foreign object", we calculated a  $p < 0.0001$ . Hence, proofing a significant change in the average RTAT.

## 4. Discussion

Our clinical workflow simulations demonstrated that a significant reduction of average RTAT for critical findings in CXRs can be achieved by an intelligent worklist prioritization using

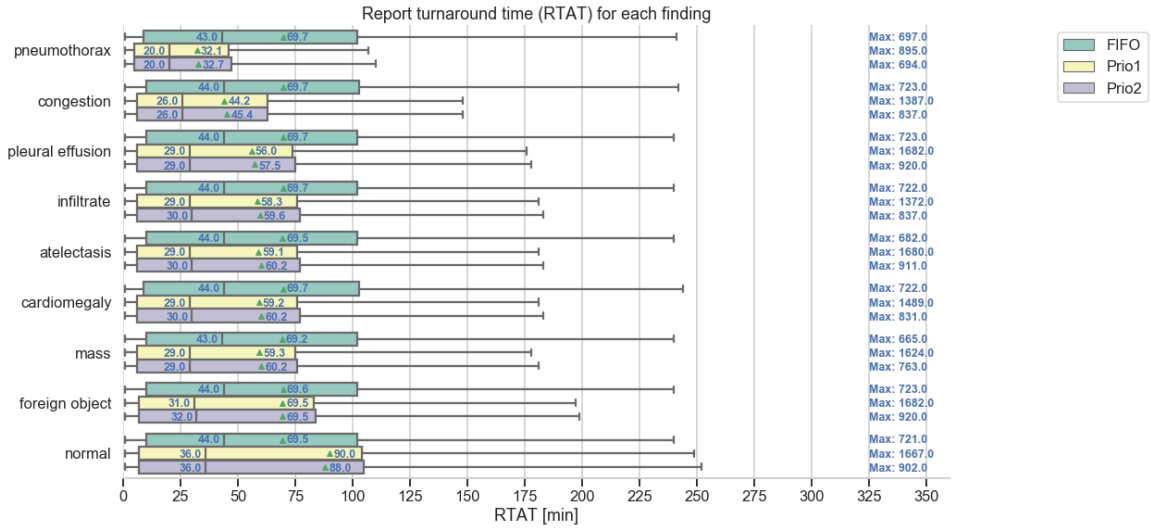


Figure 6: Report turnaround times (RTAT) for all eight pathological findings as well as for normal examinations on the basis of three different simulations: FIFO (green), Prio1 (yellow) and Prio2 with a maximum waiting time (light purple). The green triangles mark the average RTAT, while the vertical lines are marking the median RTAT.

Table 2: Finding prevalence in CXRs at the UKE (approximation by 300 samples from February 2019). The table is ordered by finding urgency. We present results in the style (avg / max) [minutes] for each simulation.

Finding	FIFO	Prio1	Prio2	Perfect
Pneumothorax	69.7 / 697	32.1 / 895	32.7 / 694	26.8 / 222
Congestion	69.7 / 723	44.2 / 1387	45.4 / 837	31.5 / 354
Pleural effusion	69.7 / 723	56.0 / 1682	57.5 / 920	41.8 / 790
Infiltrate	69.7 / 722	58.3 / 1372	59.6 / 837	44.6 / 1268
Atelectasis	69.5 / 682	59.1 / 1680	60.2 / 911	45.0 / 1317
Cardiomegaly	69.7 / 722	59.2 / 1489	60.2 / 831	45.3 / 1317
Mass	69.2 / 665	59.3 / 1624	60.2 / 763	44.9 / 1317
Foreign Object	69.6 / 723	69.5 / 1682	69.5 / 920	69.7 / 1336
Normal	69.5 / 721	90.0 / 1667	88.0 / 902	114.3 / 1336

a CNN. Furthermore, we showed that the problem of false negative predictions of an AI system can be significantly reduced by introducing a maximum waiting time.

This was proven in a realistic clinical scenario, as all simulations were based on representative retrospective data from the university hospital. By extracting discrete distributions of CXR acquisition rate as well as radiologists reporting time, the temporal sequence of a working day could be recreated precisely.

As in other application areas, the question is what error rates we can ethically and legally tolerate before CNNs can be used in patient care. For intelligent worklist prioritization, we have shown that we can easily reduce the average RTAT at the expense of individual cases that are classified as false negative and therefore reported much later than the current FIFO principle. While it was questionable whether this overall improvement outweighed the individual cases, we have shown in our Prio2-simulation that the definition of a maximum waiting time, after which all examinations with the highest urgency are assigned, solves this problem. For the most critical finding (i.e. pneumothorax), the maximum RTAT was reduced to the current standard while preserving the significant reduction of the average RTAT.

The comparison in Table 2 shows that state-of-the-arte CNNs can almost reach the upper limit of an in intelligent worklist prioritization for the average RTAT. On the other hand, for the maximum RTAT, it reveals again the problem of false negative prediction. Ideally, a perfect classification algorithm could reduce the maximum RTAT to 222 min for pneumothorax. Which, is a substantial improvement over the standard maximum with 697 min.

Besides the possible improvement in diagnostic workflow by a CNN, it should be stated that only a timely and reliable communication of the discovered findings from the radiologist to the referring clinician ensures that patients receive the clinical treatment they need.

Unlike previous publications [7] we included in- as well as outpatients, as in the daily reporting routine at the university hospital all CXRs are sorted into one worklist. Furthermore, we observed substantially shorter backlogs of unreported examinations compared to published data from the United Kingdom.

In healthcare systems where patients and referring physicians are waiting for reports up to days or weeks or have limited access to expert radiologists at all, the benefit of a worklist prioritization could obviously be even greater than in countries with a well-developed health system. The longer reporting backlogs, the more likely it is that referring physicians will try to rule out critical findings in CXRs themselves. Nevertheless, subtle findings with potentially large clinical impact (e.g. pneumothorax) that postpone the discovery by a radiologist to an irresponsible period of time could be overlooked in this way.

One limitation of our study is that the Indiana dataset, which “ChestXCheck” was trained on, mainly included outpatients in contrast to the predominantly stationary patient collective of the hospital. Therefore, the performance of our algorithm, which was already strong compared to other publications [10], could even be improved by collecting more specific training data for further studies. However, we note that the priority-based scheduling algorithm developed in this work is generic and can use any CNN that classifies X-ray pathologies. If the CNN classifier is improved, the scheduling algorithm will directly benefit from that.

In the future, we want to include more pathologies and different degrees of manifestation to further improve the gain of an intelligent worklist prioritization. While we only focused on the eight most common findings in a CXR at the university hospital and ranked them according, a large atelectasis for example can put patients health more at risk than a small pleural effusion.

Overall, the application of intelligent worklist prioritization by a CNN shows great potential to optimize clinical workflows and can significantly improve patient safety in the future. Our clinical workflow simulations suggested that triaging tools should be customized on the basis of local clinical circumstances and needs.

## References

- 1.) Reiner BI. Innovation Opportunities in Critical Results Communication: Theoretical Concepts. *Journal of digital imaging*. 2013 Aug 1;26(4):605-9.
- 2.) Hanna D, Griswold P, Leape LL, Bates DW. Communicating critical test results: safe practice recommendations. *The Joint Commission Journal on Quality and Patient Safety*. 2005 Feb 1;31(2):68-80.
- 3.) Singh H, Arora HS, Vij MS, Rao R, Khan MM, Petersen LA. Communication outcomes of critical imaging results in a computerized notification system. *Journal of the American Medical Informatics Association*. 2007 Jul 1;14(4):459-66.
- 4.) Berlin L. Statute of limitations and the continuum of care doctrine. *American Journal of Roentgenology*. 2001 Nov;177(5):1011-6.
- 5.) The Joint Commission. 2020 National Patient Safety Goals. Accessed November 5, 2019. Available from: [http://www.jointcommission.org/standards\\_information/npsgs.aspx](http://www.jointcommission.org/standards_information/npsgs.aspx)
- 6.) Rachh P, Levey AO, Lemmon A, Marinescu A, Auffermann WF, Haycock D, Berkowitz EA. Reducing STAT portable chest radiograph turnaround times: a pilot study. *Current problems in diagnostic radiology*. 2018 May 1;47(3):156-60.
- 7.) Gaskin CM, Patrie JT, Hanshew MD, Boatman DM, McWey RP. Impact of a reading priority scoring system on the prioritization of examination interpretations. *American Journal of Roentgenology*. 2016 May;206(5):1031-9.
- 8.) Yaniv G, Kuperberg A, Walach E. Deep learning algorithm for optimizing critical findings report turnaround time. In SIIM (Society for Imaging Informatics in Medicine) Annual Meeting 2018.
- 9.) Annarumma M, Withey SJ, Bakewell RJ, Pesce E, Goh V, Montana G. Automated triaging of adult chest radiographs with deep artificial neural networks. *Radiology*. 2019 Jan 22;291(1):196-202.
- 10.) Baltruschat IM, Nickisch H, Grass M, Knopp T, Saalbach A. Comparison of deep learning approaches for multi-label chest X-ray classification. *Scientific reports*. 2019 Apr 23;9(1):6381.
- 11.) Baltruschat IM, Steinmeister L, Ittrich H, Adam G, Nickisch H, Saalbach A, von Berg J, Grass M, Knopp T. When does Bone Suppression and Lung Field Segmentation Improve Chest X-Ray Disease Classification?. In 2019 IEEE 16th International Symposium on Biomedical Imaging (ISBI 2019) 2019 Apr 8 (pp. 1362-1366). IEEE.
- 12.) Wang X, Peng Y, Lu L, Lu Z, Bagheri M, Summers RM. Chestx-ray8: Hospital-scale chest x-ray database and benchmarks on weakly-supervised classification and localization

of common thorax diseases. InProceedings of the IEEE conference on computer vision and pattern recognition 2017 (pp. 2097-2106).

13.) Demner-Fushman D, Kohli MD, Rosenman MB, Shooshan SE, Rodriguez L, Antani S, Thoma GR, McDonald CJ. Preparing a collection of radiology examinations for distribution and retrieval. *Journal of the American Medical Informatics Association*. 2015 Jul 1;23(2):304-10.

14.) Gooen A, Deshpande H, Harder T, Schwab E, Baltruschat I, Mabotuwana T, Cross N, Saalbach A. Deep Learning for Pneumothorax Detection and Localization in Chest Radiographs. *arXiv preprint arXiv:1907.07324*. 2019 Jul 16.

15.) Ondategui-Parra S, Bhagwat JG, Zou KH, Gogate A, Intriere LA, Kelly P, Seltzer SE, Ros PR. Practice management performance indicators in academic radiology departments. *Radiology*. 2004 Dec;233(3):716-22.